J Sol-Gel Sci Technol
DOI 10.1007/s10971-011-2622-5

ORIGINAL PAPER

Synthesis and structural study of ethylmethylsilanediol by quantum chemical calculations and IR and Raman spectroscopies

M. P. G. Rodríguez Ortega · M. Montejo · A. Marchal Ingraín · F. Márquez · J. J. López González

Received: 6 July 2011 / Accepted: 27 October 2011

Abstract The intrinsic instability of small alkylsilanediols and their propensity toward self-condensation have been the main determiners of the scarce number of experimental works dealing with their synthesis and vibrational characterization. This is the case of the title compound, ethylmethylsilanediol (EMSD), which preparation and purification is, to the best of our knowledge, firstly reported in the present work. Hence, we also report the first records of the IR and Raman spectra of the molecule that have been thoroughly analyzed and completely assigned with the support of DFT calculations. Further, as a previous step of the vibrational assignment, we accomplished a thorough conformational analysis that allowed indentifying five conformations that represent minima on the potential energy surface (PES) of the molecule, depending on the different arrangement that both, the alkyl side chain and the –OH groups, can adopt. Finally, natural bond orbital (NBO) calculations were implemented to justify the stability order and the calculated geometries for the set of conformers in terms of the stabilization derived from the anomeric effect.

Keywords Ethylmethylsilanediol · Vibrational spectrum · Synthesis · Molecular structure · Sol–gel intermediates

M. P. G. Rodríguez Ortega · M. Montejo · F. Márquez · J. J. López González (✉)
Physical and Analytical Chemistry Department, University of Jaén, Campus Las Lagunillas, 23071 Jaén, Spain
e-mail: jjlopez@ujaen.es

A. Marchal Ingraín
Inorganic and Organic Chemistry Department, University of Jaen, Campus Las Lagunillas, 23071 Jaen, Spain

1 Introduction

Silanols are known intermediates in the sol–gel reactions of organosilicon compounds, aimed to obtain oxidic (SiO_2 based) materials of industrial interest [1]. The potential use of IR and Raman spectroscopies in the monitoring of these processes makes necessary a deep knowledge of the vibrational spectrum of precursors (normally alkoxysilanes) and intermediates of the reaction. This fact, among others, has motivated the theoretical and/or experimental study of the vibrational spectra of several relatively simple alkylsilanols [2–15]. In the case of silicon gem-diols, such as the title molecule, their intrinsic instability (which is greater in systems with small substituents) has made their synthesis and experimental characterization to be a challenging task and, consequently, only those silanediols with substituents bulky enough have been successfully synthesized [16]. Further, the interest in geminal silanediols is also being spread due to the biological role of some peptidomimetics containing the $–Si(OH)_2$ group (silicon bioisosteres) [17–20], that have proven activity as inhibitors of some aspartyl and metalloproteases (such as ACE, VIH, etc.) [21, 22].

In the present work, we report the synthesis and the joint theoretical and experimental structural characterization of a relatively small silanediol, namely ethylmethylsilanediol (EMSD), including the first vibrational records of the IR and Raman spectra of the species, which have been thoroughly analysed and completely assigned on the basis of a previous conformational analysis of the molecule, which allowed identifying five different molecular conformations representing minima in the potential energy surface (PES) of the molecule.

The results of this work may help in the monitoring, using optical spectroscopies, of the sol–gel processes of

Journal : Large 10971 | Dispatch : 4-11-2011 | Pages : 10
Article No. : 2622 | LE | TYPESET
MS Code : JSST2488 | CP | DISK

organosilicon compounds and, specifically, in those involving gem-diolic intermediates.

2 Materials and methods

2.1 Synthesis

Ethylmethylsilanediol was prepared in 61% yield from commercial dichloro(ethyl)methylsilane using the procedure reported by Cella et al. [23]. This procedure is a modification of a previously procedure reported by Takiguchi [24]. In Takiguchi's procedure, the appropriate chlorosilane dissolved in ether is added at 0 °C to a mixture of ether, aniline (1.0 equivalents per SiCl), water (1.0 equivalents per SiCl) and enough acetone to make the mixture homogeneous. The desired silanol products are then isolated by filtration to remove aniline hydrochloride, followed by evaporation of the ether and rinsing of the products with pentane to remove any higher oligomers formed during the hydrolysis. Although Takiguchi's procedure provides good yields of sensitive silanols and silanediols, the products are often unstable to storage when trace amounts of residual aniline are present. The immiscibility of aniline and pentane precludes its removal during the washing step. Therefore, when employing this method, exact stoichiometry is critical. Triethylamine used in Cella's procedure offers a number of advantages over aniline as an HCl acceptor in this procedure. Its volatility and solubility in pentane/hexane ensure its complete removal from the silanol products during work-up. It can thus be used in a slight excess during the hydrolysis step, avoiding any possibility of excess acid at the end of the reaction. Consequently, silanols and silanediols, obtained using this modified procedure, were found to be stable to storage for months in the freezer without deterioration according to NMR data.

2.1.1 Experimental procedure

Dichloro(ethyl)methylsilane (2.8 g, 20 mmol) in 30 mL of ethyl ether was added dropwise with stirring to a 0 °C solution consisting of 4.0 g of triethylamine (40.2 mmol, 2.01 equivalents), 0.8 g of water (43 mmol, 2.15 equivalents), 70 mL of ethyl ether and enough acetone (about 150 mL) to provide homogeneity. Addition of chlorosilane was complete in 1.0 h. Following addition the solution was allowed to stir for an additional 30 min at 0 °C. The triethylamine hydrochloride was removed by vacuum filtration and the filtrate was concentrated to one tenth of its volume by rotary evaporation. At this point an excess of hexane was added to the flask and rotary evaporation continued. The solid was collected by filtration and washed with cold hexane to remove any residual triethylamine. Recrystallization from hexane—ethyl ether afforded Ethylmethylsilanediol (1.3 g, 61%) as a white solid. m.p. 74–75 °C; ^{1}H NMR (400 MHz, DMSO-d_6, 25°C) δ (ppm): 5.68 (s, 2, OH); 0.87 (t, $J = 7.8$ Hz, 3H, CH_3); 0.36 (q, $J = 7.8$ Hz, 2H, CH_2); −0.10 (s, 3H, CH_3); ^{13}C NMR (DMSO-d_6): 8.37 (CH_3); 6.83 (CH_2); −1.62 (CH_3).

2.2 Vibrational spectra

The record of the IR spectra of the samples in solid phase was carried out using KBr pellets and thin films. For the preparation of the thin films, 20 µL of a solution of EMSD in acetone (0.1 M) were deposited in a CsI window. Afterwards, the solvent was evaporated under anhydrous condition. IR spectrum of the solid deposition on the window was recorded in the 400–4,000 cm^{-1} range using a FT-IR Jasco 4100 spectrophotometer, equipped with a Globar source and a DTGS detector. IR spectrum of the sample in KBr pellet was recorded in the 300–4,000 cm^{-1} range using a FT-IR Bruker Vector 22 spectrophotometer, equipped with a Globar source, CsI optics and a DTGS detector. Both spectra were obtained with a resolution of 1 cm^{-1} and 100 scans.

The Raman spectrum of the pure sample was recorded with a Bruker RF100/S FT-Raman spectrometer, equipped with a Nd: YAG laser (excitation line 1,064 nm) and a cooled Ge detector at liquid nitrogen temperature. The spectrum was recorded with a resolution of 1 cm^{-1} and 100 scans were used to improve the signal-to noise ratio.

3 Theory

3.1 Computational details

Ab initio and DFT calculations reported were performed using the Gaussian 03 suite of programs [25]. Geometry optimizations and frequency calculations for the different conformers of the EMSD molecule were carried out using the Becke's three-parametric hybrid exchange functional [26] combined with the Lee–Yang–Parr correlation functional [27], (B3LYP) and the second order Möller- Plesset perturbation theory [28] method (MP2), in conjunction with the 6-31G* [29], 6-311++G** [30] and aug-cc-pVTZ [31] basis sets (the last only in the case of B3LYP calculations). Geometry optimizations were tighten using the keywords opt = VTight, SCF = Tight and Int = Ultrafine (in the case of DFT calculations). These options set the threshold of the RMS force criterion to 1×10^{-6} during the geometry optimization and scale the remaining criteria accordingly. Each stationary point obtained was

Journal : Large 10971 Dispatch : 4-11-2011 Pages : 10
Article No. : 2622 LE TYPESET
MS Code : JSST2488 CP DISK

characterized by the vibrational frequencies computation at the same level of theory.

The force fields obtained in cartesian coordinates at the B3LYP/aug-cc-pVTZ level were transformed into a set of natural internal coordinates [32] in order to obtain a more comprehensive description of the PEDM (Potential Energy Distribution Matrix). The force field transformation into natural valence coordinates and normal-mode analyses were performed using the MOLVIB [33, 34] program.

Natural bond orbital NBO [35] calculations were accomplished using the NBO v3.1 [36] as implemented in Gaussian 03.

4 Results and discussion

4.1 Theoretical conformational analysis and molecular structure

To the best of our knowledge, this is the first report of the molecular structure of the title compound from either a theoretical or experimental point of view.

Searches for the conformers of EMSD were performed in two steps. Firstly, we performed a conformational analysis considering the *gauche* (g) or *anti* (a) orientation that the ethyl groups can adopt respect to the Si–O bonds [37]. In such systems, the possible values of the C–C–Si–O dihedral angle with respect to the remaining Si–O bond are 180° (a), +60° (g+) and −60° (g−) as shown in Fig. 1. In this way, three different arrangements of the ethyl group were considered.

For each of these structures, a relaxed scan of one of the C–Si–O–H dihedral angles was performed at the B3LYP/6-31G* level, in order to evaluate the possible relative orientations that the OH groups would adopt. As shown in Fig. 2, these scans present two minima. The local minimum corresponds to a *gauche-trans* (*gt*) conformation of the hydroxyl groups (which H–O–O–H dihedral angle is close to 80°), whereas the global minimum corresponds to a structure with the OH groups in *gauche–gauche* (*gg*) arrangement, tilted from the OSiO plane by approximately 60°. These two conformations of the hydroxyls groups are essentially the same than those found by our research group for a closely related molecule previously studied, i.e. dimethylsilanediol (DMSD).

In order to determine if these structures represent real minima on the PES of the molecule, their vibrational spectra were calculated, rendering no imaginary frequencies in the case of the conformations detected in scans I and II and the global minimum in scan III. On the contrary, the calculation yielded one imaginary frequency for the local minimum in scan III, which corresponds to the Si–O torsional deformation mode. Therefore, this structure was discounted. Summarizing, five conformers were finally identified and characterized as real minima on the PES of EMSD as shown in Fig. 3. Note that the pairs CI and CI′, and CII and CII′ differ on the orientation of the OH groups, keeping the same arrangement of the alkyl chains.

The calculated geometrical parameters of CI, CII and CIII are very similar. The more significant differences between these three conformers are found for the dihedral angles C–C–Si–O, which are different depending on the *gauche* (g+ or g−) or *anti* position adopted for the ethyl group respect to the Si–O bonds. Thus, for CI the value of the dihedral angles C_6–C_5–Si_1–O_2 and C_6–C_5–Si_1–O_3 are 178.8° and 59.2° (B3LYP/aug-cc-pVTZ), respectively. For CII and CIII, these dihedral angles are −59.8° and −179.5°, and 61.1° and −58.6°, respectively. On the other hand, for conformers I and I′, as well as for conformers II and II′, the main differences lie on the bond distances and bond angles that are affected by the OH arrangement. For instance, both Si–O bond distances are almost the same in CI, CII and CIII, whereas for CI′ and CII′ Si_1–O_2 bond distance is sensibly higher than Si_1–O_3 bond. The same goes for the Si–C bond distances of conformers I′ and II′.

These differences in bond distances and angles between conformers I and its counterpart I′, as well as between conformers II and II′, can be explained on the basis of the anomeric effect (negative hyperconjugation of the lone pairs of the oxygen atoms), which only take place when the –OH groups are in *gauche* orientations respect to the Si–O bond. Thus, the influence of the hyperconjugative effects in

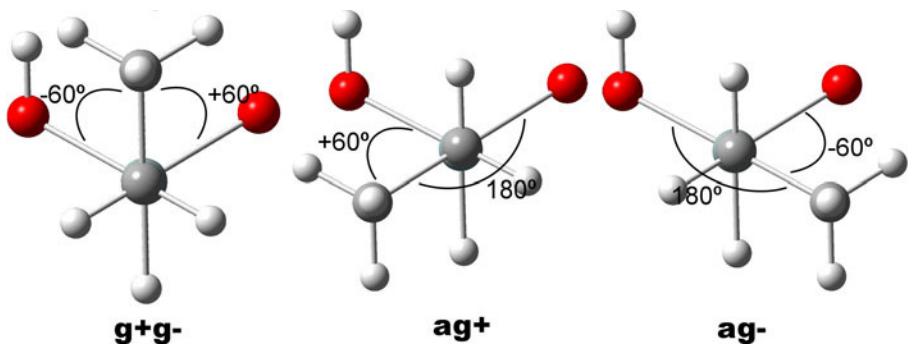

Fig. 1 Different conformations adopted by the ethyl group in a generic silanediol system

Journal : Large 10971 | Dispatch : 4-11-2011 | Pages : 10
Article No. : 2622 | LE | TYPESET
MS Code : JSST2488 | CP | DISK

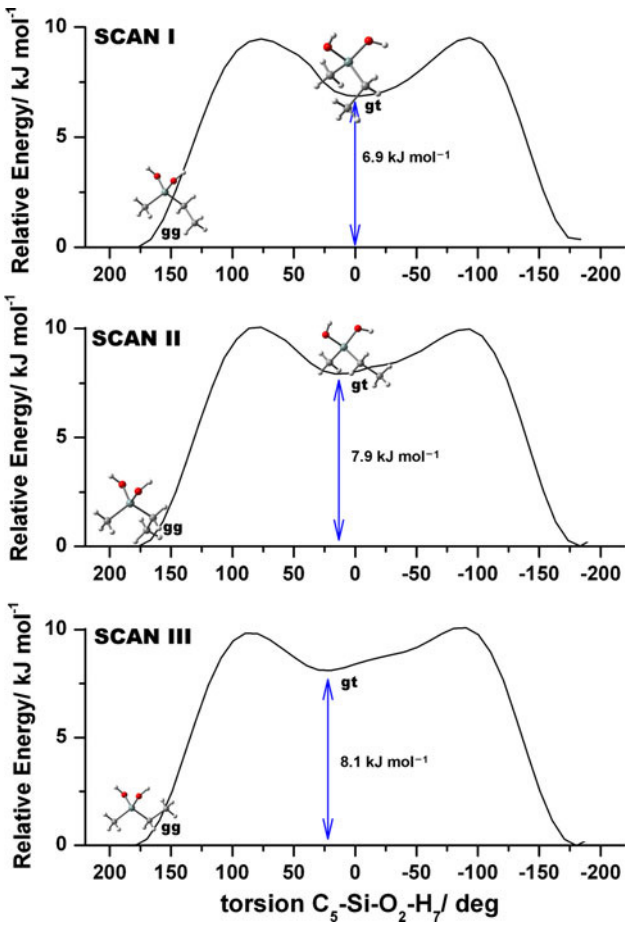

Fig. 2 Plots of the relaxed scans of the C–Si–O–C dihedral angle obtained for the three possible alkyl chains arrangements in the EMSD molecule (B3LYP/6-31G*)

the calculated geometries was studied in the frame of NBO population analysis carried out for the series of conformers (B3LYP/aug-cc-pVTZ).

In Table 1, the electronic populations of the so-called lone pair orbitals of the oxygen atoms and the σ and σ^* orbitals of the SiO and SiC bonds are reported. As can be seen, the occupation of the antibonding orbital corresponding to SiO_2 bond is higher than in the SiO_3 bond of conformers I′ and II′ (both with a *gt* arrangement of the hydroxyl groups), which is consistent with the lengthening of the SiO_2 bond in these structures. Besides, the antibonding orbital σ^*_{SiC4} is appreciably less occupied than the antibonding orbital σ^*_{SiC5}, and thus, the SiC_4 bond is shorter. Furthermore, unlike *gt* conformers the electronic populations of the bonding orbitals σ_{SiO2} and σ_{SiO3}, and of the bonding orbitals σ_{SiC4} and σ_{SiC5} in *gg* conformers, are almost equal.

Since high populations in the antibonding orbitals lead to a lengthening of the bonds, these mentioned differences may explain the disparity in the calculated equilibrium distances for the same type of bond within one molecule.

Due to the fact that the anomeric effect is favored when the hydroxyl group is in *gauche* arrangement, this electronic transfer can take place from both –OH groups in the case of *gg* conformers, and only from one of the –OH groups in *gt* conformers. Table 2 shows the magnitude of the interaction between the lone pairs of one of the oxygen atoms and the antibonding SiC and SiO bonds of each conformer of EMSD. As can be seen, the sum of the magnitude of all interactions between the lone pairs of both oxygen atoms and the mentioned antibonding orbitals is 6.4 kJ/mol (average) higher in *gg* conformers than in *gt* conformers. For closely related systems, as the previously studied dimethylsilanediol molecule, has been proven that lower contributions to the stabilizing anomeric effect could even justify the instability of some structures. This could be the case of the local minimum in scan III which, in fact, do not represent minimum on the PES of EMSD.

These results confirm that the *gg* conformations are strongly favored since the electronic delocalizations of the oxygen electron lone pairs are higher in such systems. Also, these results are consistent with the theoretical geometrical parameter values found for the five conformers and their predicted order of stabilities in the gas phase, discussed below.

Numerical values of calculated ΔG, ΔG^* and ΔE_o (see footnote on Table 3 for definition) obtained with the different theoretical methods are summarized in Table 3. As can be seen, the energy difference between the five conformers decrease with the increase of the basis set size, as shown in Fig. 4.

Their relative populations in the gas phase (at room temperature) were calculated theoretically (B3LYP/aug-cc-pVTZ) from the ΔE_o values, using the Boltzmann distribution equation. Conformers CI′ and CII′ (*gt* arrangement of hydroxyl groups) are estimated to be present in lower proportion than *gg* conformers, being their theoretical gas phase population 16.2 and 15.2%, respectively. Conformer III is estimated to have the higher theoretical population in gas-phase (23.2% B3LYP/aug-cc-pVTZ). Conformers CI and CII are calculated to represent the 22.4 and 23.0%, respectively, of the total sample composition.

4.2 Vibrational study

The IR spectra of the solid phase (KBr pellet and thin film) and the Raman spectrum of the pure solid EMSD are shown in Fig. 5. The observed vibrational bands and their relative intensities are listed in Table 4 along with their proposed assignments to the normal modes of the three main conformers of EMSD.

For the sake of clarity, throughout this discussion, and unless otherwise stated, we will refer to the experimental bands observed in the IR spectra of the KBr pellet.

Journal : Large 10971 Dispatch : 4-11-2011 Pages : 10
Article No. : 2622 LE TYPESET
MS Code : JSST2488 CP DISK

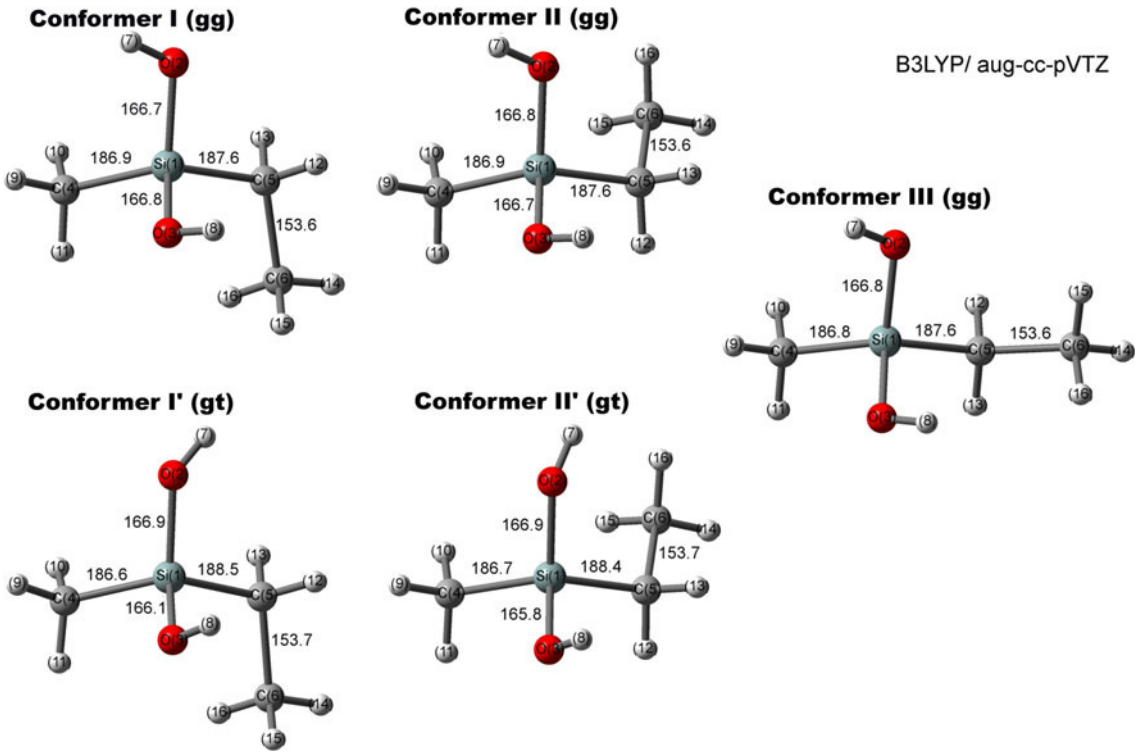

Fig. 3 Molecular structures and atom numbering for the five conformers of EMSD

Table 1 B3LYP/aug-cc-pVTZ NBO electronic populations (in a.u.) of the lone pair (LP) orbitals of the oxygen atoms and the σ^* orbitals of the SiC bonds in EMSD

Orbital	Electronic population (a.u)				
	CI	CII	CIII	CI′	CII′
σ SiO_2	1.98628	1.98645	1.98636	1.98608	1.98628
σ SiO_3	1.98643	1.98635	1.98631	1.98689	1.98672
σ SiC_4	1.97158	1.97159	1.97140	1.97180	1.97182
σ SiC_5	1.95976	1.95985	1.95951	1.96103	1.96061
LP(1) O_2	1.97015	1.97032	1.97010	1.97184	1.97020
LP(1) O_3	1.97086	1.97054	1.97026	1.97001	1.96973
LP(2) O_2	1.93640	1.93641	1.93686	1.93904	1.94201
LP(2) O_3	1.93640	1.93632	1.93665	1.93789	1.93809
σ^* SiO_2	0.07233	0.07618	0.07580	0.06665	0.07009
σ^* SiO_3	0.07621	0.07258	0.07515	0.06369	0.05524
σ^* SiC_4	0.05746	0.05719	0.05470	0.05913	0.06090
σ^* SiC_5	0.06157	0.06046	0.06222	0.07172	0.07314

4.2.1 Region between 3,300 and 1,200 cm^{-1}

The vibrational assignment of this spectral region has been carried out using CI, CII and CIII conformers as a reference, since their population amounts to 68.6% (B3LYP/aug-cc-pVTZ) of the sample composition in gas phase.

Nevertheless, for the five conformers into study, the theoretical values of the normal modes falling in the 3,200–1,200 cm^{-1} region are very close and, in all cases, reasonably reproduce the experimental profile, considering the expected theoretical/experimental deviations derived from the use of the harmonic approximation in the theoretical methods.

Starting from the higher wavenumbers region, IR spectra of EMSD of both KBr pellet and thin film show a very strong and broad band centered at 3,200 cm^{-1} which

Journal : Large 10971 Dispatch : 4-11-2011 Pages : 10
Article No. : 2622 LE TYPESET
MS Code : JSST2488 CP DISK

Table 2 Magnitude (in kJ mol^{-1}) of the interaction energies between the two lone pairs orbitals of the oxygen atoms and the σ^* orbitals of the SiC and SiO bonds in EMSD calculated at the B3LYP/aug-cc-pVTZ level

Interaction	$E^{(2)}$ (kJ mol^{-1})				
	CI	CII	CIII	CI′	CII′
LP(1) O_2 → σ^* SiO_3	4.39	3.81	5.19	7.20	11.67
LP(1) O_3 → * SiO_2	4.81	4.48	4.69	10.17	9.21
LP(1) O_2 → * SiC_4	10.17	10.30	9.00	–	–
LP(1) O_3 → * SiC_4	12.22	12.10	12.01	11.38	11.51
LP(1) O_2 → * SiC_5	12.77	12.72	12.77	14.32	13.56
LP(1) O_3 → * SiC_5	8.58	8.58	8.58	3.68	7.28
LP(2) O_2 → * SiO_3	40.06	40.81	37.84	24.74	14.61
LP(2) O_3 → * SiO_2	38.64	39.85	39.01	23.48	24.99
LP(2) O_2 → * SiC_4	19.46	18.54	21.56	30.68	34.28
LP(2) O_3 → * SiC_4	–	–	–	3.31	2.76
LP(2) O_2 → * SiC_5	–	–	–	2.34	7.37
LP(2) O_3 → * SiC_5	20.26	19.42	20.86	30.68	29.72
$\sum$	171.36	170.61	170.51	161.98	166.96

Table 3 Relative Gibbs free energies (ΔG and ΔG*) and ΔE_o energies of the five conformers of EMSD calculated with the B3LYP and MP2 methods and the different basis sets employed

		ΔG (kJ mol^{-1})			ΔG* (kJ mol^{-1})			ΔE_o (kJ mol^{-1})		
		6-31+G*	6-311++G**	aug-cc-pVTZ	6-31+G*	6-311++G**	aug-cc-pVTZ	6-31+G*	6-311++G**	aug-cc-pVTZ
B3LYP	CI	2.93	2.80	1.59	0.84	0.46	0.46	0.75	0.50	0.38
	CII	2.76	1.67	0.71	0.38	0.25	0.12	0.42	0.25	0.08
	CIII	0.00	0.00	0.00	0.00	0.00	0.00	0.00	0.00	0.00
	CI′	14.73	14.86	4.73	8.20	6.82	5.86	5.65	4.77	3.72
	CII′	11.09	15.06	2.5	8.75	7.53	6.48	5.90	5.19	4.39
MP2	CI	2.43	3.14	–	0.08	0.29	–	0.54	0.50	–
	CII	0.79	0.42		0.00	0.08		0.00	0.00	
	CIII	0.00	0.00		1.30	0.00		0.00	0.00	
	CI′	15.53	18.67		9.92	6.40		6.03	5.02	
	CII′	15.53	19.34		8.62	7.53		6.03	5.73	

Energy values in kJ mol^{-1}

ΔG* stands for the Gibbs free energy values obtained when the entropic corrections to the low frequencies modes of vibrations are subtracted from the Gibbs free energies calculated

$E_o = E_e + ZPE$

can be attributed to the OH stretching mode of the hydrogen-bond network.

Between 2,960 and 2,880 cm^{-1}, we observe five intense bands in the IR spectrum of the sample, corresponding to the symmetric and asymmetric stretching modes of C–H bonds of methyl and methylene groups, as reported in Table 4.

The bands observed between 1,470 and 1,270 cm^{-1} have been assigned to the asymmetric deformations of the methyl groups, methylene scissoring and $–CH_3$ symmetric deformations, according to their respective theoretical values (see Table 4).

Finally, the vibrational bands centered at 1,258 and 1,242 cm^{-1} have been attributed to methylene wagging and twisting of the ethyl group, respectively, also in agreement with their calculated values (Table 4).

4.2.2 Region below 1,200 cm^{-1}

Although in this region the above mentioned experimental-theoretical deviations are slighter (due to the minor anharmonic character of the normal modes appearing in this region), the spectral profile of the sample is very

Journal : Large 10971 Dispatch : 4-11-2011 Pages : 10
Article No. : 2622 LE TYPESET
MS Code : JSST2488 CP DISK

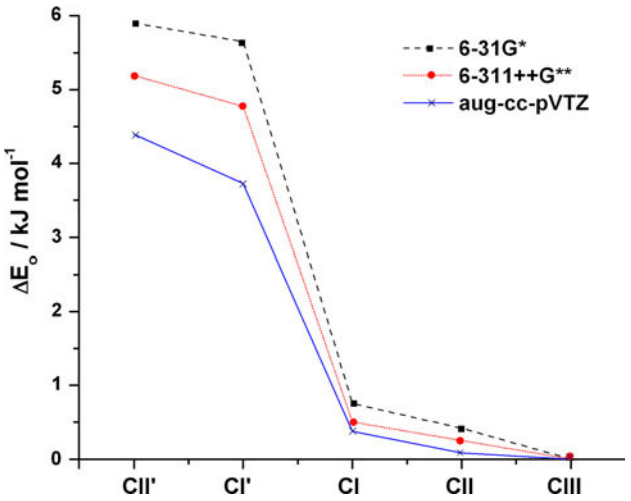

Fig. 4 Effect of increasing the basis set size on the calculated values of ΔE_o at the B3LYP level of theory

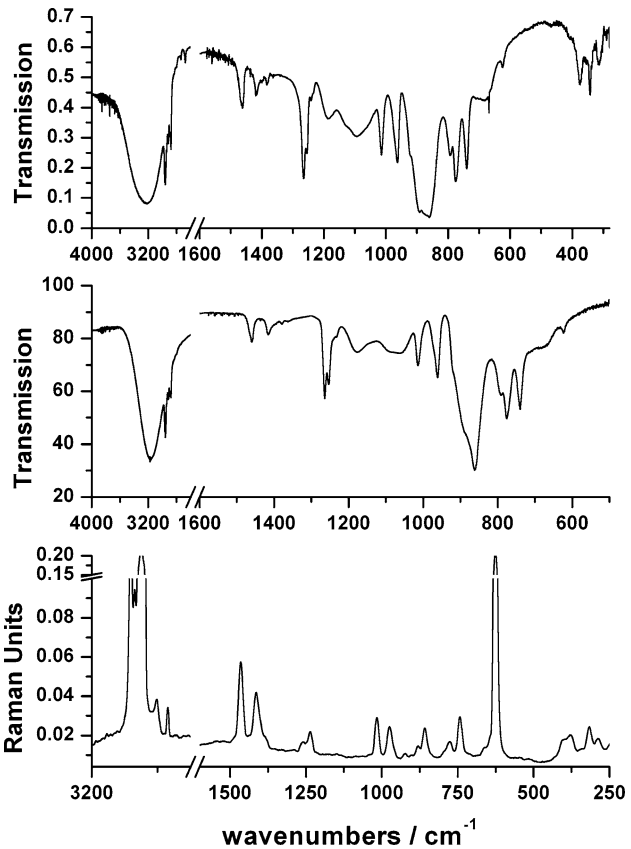

Fig. 5 Experimental IR spectra of the KBr pellet (*top*) and the thin film (*middle*) and the Raman spectrum of the solid phase (*bottom*) for EMSD

complex due to the blueshifting of some characteristic vibrational modes of the silanediol group in the hydrogen bonded network.

IR spectrum of the sample show a medium intensity band centered at 1,185 with a shoulder at 1,060 cm^{-1}, attributable to the symmetric and asymmetric –Si–O–H deformation mode of hydrogen-bonded oligomers of EMSD of different size. This supposition is supported by previous works dealing with the study of the vibrational spectra of cyclic oligomers of the silanol molecule [12, 38].

The bands appearing between 1,020 and 930 cm^{-1} have been assigned to the C–C stretching mode, $Si–CH_3$ rocking and methylene twisting, according to their theoretical values (Table 4).

The stretching mode of the Si–O bond appears as a strong band centered at 892 cm^{-1}. As was stated by previous authors [38], the slight strengthening of the Si–O bond due to the formation of hydrogen bonds produces an increase of ca. 20–40 cm^{-1} in the wavenumber of the Si–O stretching normal mode. Thus, the observed band centered at 922 cm^{-1} in the IR spectra has been assigned to the blue shifting of the Si–O stretching normal mode. This assignment is also consistent with the previously obtained results for DMSD.

The two intense bands at 861 and 793 $cm^{-}1$ have been attributed to the asymmetric and symmetric deformation modes of the –SiOH group, in agreement with theoretical calculations (Table 4).

Finally, the bands appearing in the spectral region between 800 and 600 cm^{-1} have been assigned to the methyl and methylene rockings, and to the Si–C stretching mode, according to their theoretical values that are reported in Table 4.

4.2.3 Low frequency region

The experimental bands appearing below 600 cm^{-1} have been assigned to the skeletal vibrational modes of the molecule, according to their calculated values (Table 4). Remarkably, the assignment of these vibrational bands allowed detecting the presence of more than one molecular conformation in the samples.

The theoretical IR and Raman spectra obtained averaging the weighted contributions of the three main conformers of EMSD (according to their relative populations in gas phase) is compared with the spectral profile of CI, CII and CIII in the 420–260 cm^{-1} region (above) and with the experimental IR and Raman spectra in the same region (below) in Fig. 6.

As can be seen, the bands appearing at 345 and 315 cm^{-1} in the IR and Raman spectra of the sample cannot be assigned to the main conformer (CIII), and can only be justified assuming the presence of CI and/or CII (see also Table 4). This fact evidence the conformational mixture in the samples.

Journal : Large 10971 Dispatch : 4-11-2011 Pages : 10
Article No. : 2622 LE TYPESET
MS Code : JSST2488 CP DISK

Table 4 Experimentally observed bands and theoretical frequencies (in cm^{-1}) at the B3LYP/aug-cc-pVTZ level for the three main conformers of the EMSD molecule along with the proposed assignments and the main terms of the PED for each mode

Experiment[a]			Theory			Description[b,c]
IR		Raman	B3LYP/aug-cc-pVTZ			
KBr pellet	Thin film	Solid	CI	CII	CIII	
			3873	3874	3874	νOH
			3871	3872	3872	
3200s.br	3194s.br					νOH network
2961s	2961s	2964s	3102	3103	3101	$\nu^{as}C–CH_3$
			3095	3095	3095	
2940s	2941sh	2940s	3086	3092	3090	$\nu^{as}Si–CH_3$
			3073	3074	3070	
2917s	2917s	2915sh	3042	3040	3044	$\nu^{as}CH_2$
2893w	2891m	2899s	3030	3030	3029	$\nu^{s}Si\text{-}CH_3$
2878w	2879s	2881s	3023	3024	3020	$\nu^{s}C\text{-}CH_3$
			3012	3008	3013	$\nu^{s}CH_2$
		2807w				Overtone (2 × 1415)
2740vw	2738w	2739w				Overtone (2 × 1383)
2677vw						Combination (1417 + 1265)
2491vw						Overtone (2 × 1258)
1466sh			1508	1508	1510	$\delta^{as}CCH_3$
1462m	1460m	1464w	1504	1505	1504	$\delta^{as}CCH_3$
1417w	1419sh		1464	1464	1463	$\delta^{as}SiCH_3$
1415w	1416m	1415w.br	1461	1461	1460	$\delta^{as}SiCH_3$
1383w	1379m	1380vw	1454	1452	1453	$scCH_2$
1364vw	1364 m		1418	1416	1414	$\delta^{s}CCH_3$
1265m	1264s	1265vw	1297	1297	1297	$\delta^{s}SiCH_3$
1258m	1254s	1255vw	1278	1280	1281	$waCH_2$ (ρ CH_3)
1242sh	1241vw	1246w	1262	1268	1269	tw H_2 + ρCH_2
1185m	1180m.br					Oligomers[d]
	1060sh					Oligomers[d]
1014m	1013s	1016w	1030	1030	1029	νCC + $\rho SiCH_3$
970sh	969sh	976w	984	988	986	$\rho SiCH_3$ + $twCH_2$
963m			981	980	981	νCC + $\rho SiCH_3$ + $waCH_2$
			904	904	901	δSiOH + νSiO
922sh	922sh	926vw				νSiO blueshifted
892vs	886sh	881vw	885	883	885	νSiO
861vs	861s.br	859w	876	876	877	δSiOH + νSiO
793m	792s		803	804	802	δSiOH + νSiO
776m	776s	778w	774	778	779	ρCCH_3 (δSiOH)
			770	769	766	ρCCH_3 + νSiO + δSiOH
741m	740s	743w	724	723	704	νSiC ($\rho SiCH_3$)
690w.br			672	674	692	ρCH_2
624w	624w	626vs	607	609	612	νSiC
405vw		**405**sh	**384**		**386**	$waSiC_2$ + scCCSi
375w		**380**vw		**368**	**363**	scOSiO + scCCSi
345w		**350**vw	**332**	**345**		τSiO + scCCSi + ρSiC_2
315w		**317**vw	**309**	**309**		$waSiC_2$ + τCC

Journal : Large 10971 Dispatch : 4-11-2011 Pages : 10
Article No. : 2622 LE TYPESET
MS Code : JSST2488 CP DISK

Table 4 continued

Experiment[a]			Theory			Description[b,c]
IR		Raman	B3LYP/aug-cc-pVTZ			
KBr pellet	Thin film	Solid	CI	CII	CIII	
282w		**288**vw	278	274	284	$\rho SiC_2 + \tau SiO + scCSiC$
					276	
		240vw	240	239	235	$twSiC_2 + \tau SiO + \rho SiC_2$
			236	231	231	
			213	215	216	$twSiC_2 + scOSiO$
		178vw	126	171	179	$\tau CC + twSiC_2 + scCSiC$
		140vw	142	142	137	τSiC
			135	133	132	$scCSiC + scCCSi$
			62	62	60	τSiC

The bands that prove the presence of more than one conformer are shown in bold

[a] *vs* very strong, *s* strong, *m* medium, *w* weak, *vw* very weak, *sh* shoulder, *br* broad

[b] Only shown contributions higher than 15%

[c] *Symbols used*: *v* stretching, δ deformation, ρ rocking, τ torsion. *sc* scissoring, *tw* twisting, *wa* wagging. Superscripts "s" and "as" denote symmetric and asymmetric motions

[d] See text for explanation

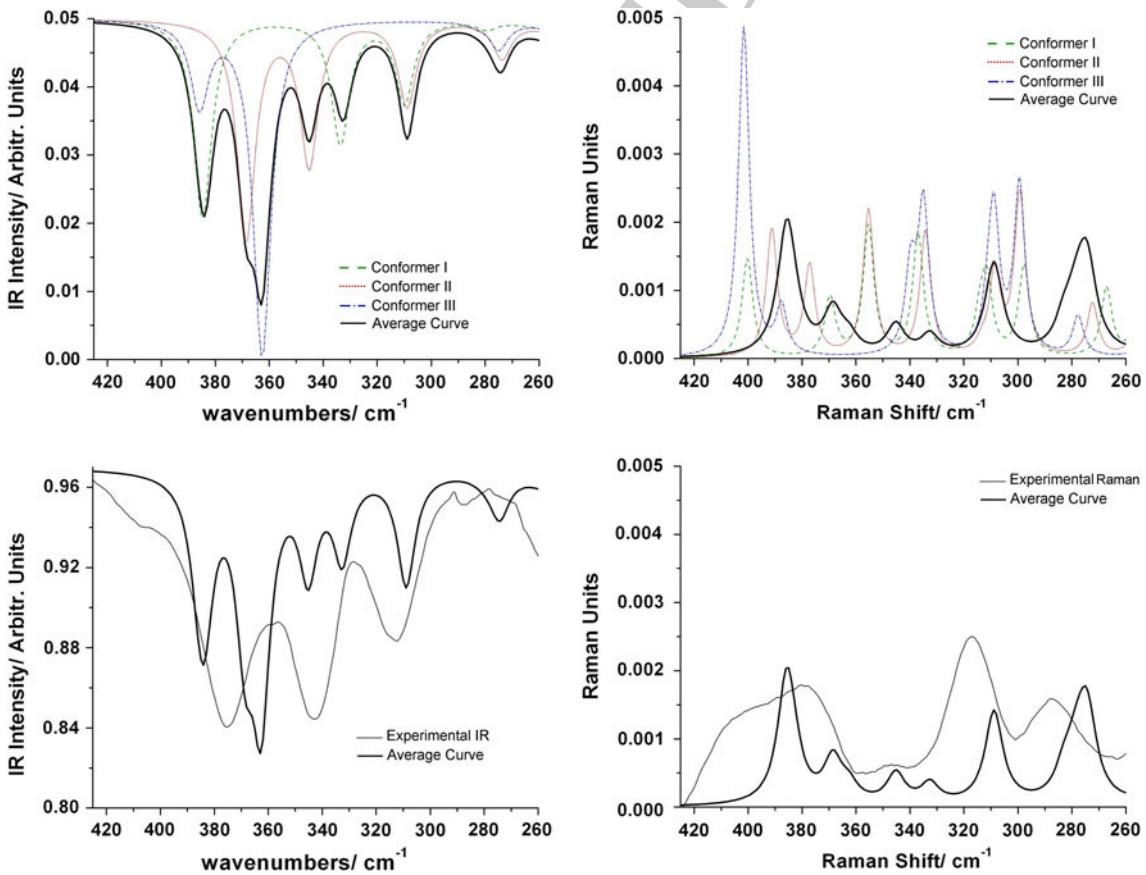

Fig. 6 Theoretical IR and Raman spectra obtained averaging the weighted contributions of the three main conformers of EMSD compared with the theoretical spectral profile of CI, CII and CIII (*above*) and with the experimental IR and Raman spectra (*below*) in the 420–260 cm^{-1} region

Journal : Large 10971 Dispatch : 4-11-2011 Pages : 10
Article No. : 2622 LE TYPESET
MS Code : JSST2488 CP DISK

5 Conclusions

1. EMSD has been synthesized for first time, using the procedure reported by *Cella* et al., with 61% yield. The first records of the IR and Raman spectra of the molecule are also reported.
2. A thorough conformational analysis confirmed that five different molecular conformations are minima on the PES of EMSD, differing in the *anti* or *gauche* ($g+$ or $g-$) orientation of the ethyl group and in the *gg* or *gt* arrangement of the –OH groups.
3. The predicted order of stabilities and Boltzmann populations in gas phase (i.e. CIII > CII > CI > CII' > CI' at B3LYP/aug-cc-pVTZ level) are explained in terms of the stabilization of the different molecular conformations due to the anomeric effect, theoretically analyzed by NBO calculations.
4. Finally, a complete vibrational assignment, accomplished with the support of B3LYP/aug-cc-pVTZ calculations, has evidenced the occurrence of the conformational mixture in the samples.

Acknowledgments The authors thank Andalussian government for funding (FQM173, FQM182) and the CICT facilities of the University of Jaén. P.G.R.O. thanks Spanish Ministerio de Educación for a Ph.D studentship (AP2009-3949) supporting this work.

References

1. Brinker CJ, Scherer GW (1989) Sol–gel science: the physics and chemistry of sol–gel processing. Academic Press, San Diego
2. Raghavachari K, Chandrasekhar J, Frisch MJ (1982) J Am Chem Soc 104:3779–3781
3. Sauer J, Ahlrichs R (1990) J Chem Phys 93:2575–2583
4. Hill JR, Sauer J (1991) J Mol Phys 73:335–348
5. Nicholas JB, Winans RE, Harrison RJ, Iton LE, Curtiss LA, Hopfinger AJ (1992) J Phys Chem 96:10247–10257
6. Darling CL, Schlegel HB (1993) J Phys Chem 97:8207–8211
7. Stave MS, Nicholas JB (1993) J Phys Chem 97:9630–9641
8. Bleiber A, Sauer J (1995) Chem Phys Lett 238:243–252
9. Nicholas JB, Feyereisen M (1995) J Chem Phys 103:8031–8042
10. Koput J (2000) J Phys Chem A 104:10017–10022
11. Tielens F, De Proft F, Geerlings P (2001) J Mol Struct (Teochem) 542:227–237
12. Ignatyev IS, Partal F, López González JJ (2002) J Phys Chem A 106:11644–11652
13. Rouviere J, Tabacik V, Fleury G (1973) Spectrochim Acta A 29:229–242
14. Bueno AW (1980) Spectrochim Acta A 36:1059–1064
15. Ignatyev IS, Partal F, López González JJ, Sundius T (2004) Spectrochim Acta A 60:1169–1178
16. Chandrasekhar V, Boomishankar R, Nagendran S (2004) Chem Rev 104:5847–5910
17. Showell GA, Mills JS (2003) Drug Discov Today 8:551–556 (and ref. therein)
18. Eder J, Hommel U, Cumin F, Martoglio B, Gerhartz B (2007) Curr Pharm Design 13:271–285 (and ref. therein)
19. Nguyen J-T, Hamada Y, Kimura T, Kiso Y (2008) Arch Pharm Chem Life Sci 341:523–535 (and ref. therein)
20. Tsantrizos YS (2008) Acc Chem Res 41:1252–1263
21. Mutahi MW, Nittoli T, Guo L, Sieburth SMN (2002) J Am Chem Soc 124:7363–7375
22. Sieburth SMN, Chen C-A (2006) Eur J Org Chem 2:311–322
23. Cella JA, Carpenter JC (1994) J Organomet Chem 480:23–26
24. Takiguchi T (1959) J Am Chem Soc 81:2359–2361
25. Gaussian 03, Revision E 01, Frisch MJ, Trucks GW, Schlegel HB, Scuseria GE, Robb MA, Cheeseman JR, Montgomery JA, Vreven Jr T, Kudin KN, Burant JC, Millam JM, Iyengar SS, Tomasi J, Barone V, Mennucci B, Cossi M, Scalmani G, Rega N, Petersson G A, Nakatsuji H, Hada M, Ehara M, Toyota K, Fukuda R, Hasegawa J, Ishida M, Nakajima T, Honda Y, Kitao O, Nakai H, Klene M, Li X, Knox JE, Hratchian HP, Cross JB, Adamo C, Jaramillo J, Gomperts R, Stratmann RE, Yazyev O, Austin AJ, Cammi R, Pomelli C, Ochterski JW, Ayala PY, Morokuma K, Voth GA, Salvador P, Dannenberg JJ, Zakrzewski VG, Dapprich S, Daniels AD, Strain MC, Farkas O, Malick DK, Rabuck AD, Raghavachari K, Foresman JB, Ortiz JV, Cui Q, Baboul AG, Clifford S, Cioslowski J, Stefanov BB, Liu G, Liashenko A, Piskorz P, Komaromi I, Martin RL, Fox DJ, Keith T, Al-Laham MA, Peng CY, Nanayakkara A, Challacombe M, Gill PMW, Johnson B, Chen W, Wong MW, Gonzalez C, Pople JA. (2004) Gaussian Inc, Wallingford, CT
26. Becke AD (1993) J Chem Phys 98:5648–5652
27. Lee C, Yang W, Parr RG (1988) Phys Rev B 37:785–789
28. Binkley JS, Pople JA (1975) Int J Quantum Chem 9:229–236
29. Hehre WJ, Ditchfield R, Pople JA (1972) J Chem Phys 56:2257–2261
30. McLean AD, Chandler GS (1980) J Chem Phys 72:5639–5648
31. Kendall RA, Dunnning TH Jr, Harrison RJ (1992) J Chem Phys 96:6796–6806
32. Fogarasi G, Pulay P (1985) In: Durig, JR (ed) Ab initio calculations of force fields and vibrational spectra. Vibrational spectra and structure, vol 14. Elsevier, New York
33. Sundius T (1990) J Mol Struct 218:321–326
34. Sundius T (2002) Vib Spectrosc 29:89–95
35. Reed AE, Curtiss LA, Weinhold F (1988) Chem Rev 88:899–926
36. Carpenter JE, Weinhold F (1988) J Mol Struct (Theochem) 169:41–62
37. Montejo M, Partal F, Márquez F, López González JJ (2008) J Phys Chem A 112:1545–1551
38. Carteret C (2006) Spectrochim Acta A 64:670–680 (and references therein)

Journal : Large 10971 | Dispatch : 4-11-2011 | Pages : 10
Article No. : 2622 | ☐ LE | ☐ TYPESET
MS Code : JSST2488 | ☑ CP | ☑ DISK